We are IntechOpen,
the world's leading publisher of
Open Access books
Built by scientists, for scientists

6,900
Open access books available

186,000
International authors and editors

200M
Downloads

Our authors are among the

154
Countries delivered to

TOP 1%
most cited scientists

12.2%
Contributors from top 500 universities

CLARIVATE ANALYTICS

BOOK CITATION INDEX

INDEXED

WEB OF SCIENCE™

Selection of our books indexed in the Book Citation Index
in Web of Science™ Core Collection (BKCI)

Interested in publishing with us?
Contact book.department@intechopen.com

Numbers displayed above are based on latest data collected.
For more information visit www.intechopen.com

A Novel Parallel Engraving Machine Based on 6-PUS Mechanism and Related Technologies

Kong Ling-fu & Zhang Shi-hui

1. Introduction

Conventional computer engraving machine has played an important role in industries such as machinery machining, printing and dyeing and entertainment, but it has the inherent disadvantages such as cutting tool can be fed only along the fixed guideway, lower degree-of-freedom(DOF) of cutting tool, lower flexibility and mobility for machining etc. Parallel mechanism has the merits such as high mechanical stiffness, high load capacity, high precision, good dynamic performance etc (Huang,1997). According to the characteristics of parallel mechanism, it has been a hot research topic to apply parallel mechanism to the domain of future machining. By applying parallel mechanism to engraving domain, its inherent advantages can be fully exerted and the disadvantages of conventional engraving machine can be overcome or compensated. But as the special structure of parallel mechanism, the related theory and technology during its engraving is very different from that of conventional engraving machine, and it is a undeveloped research topic by now. In addition, with the development of computer network technology, the new concept and method such as network machining and manufacturing has become hot research topic(Huang & Mak,2001; Taylor & Dalton,2000; Yao & Lu,1999). A novel parallel engraving machine with six-axis linkage is proposed in this paper, which uses the 6-PUS parallel mechanism with 6-DOF as the prototype, and some key technologies such as size design, tool path planning, engraving force control and teleoperation are studied on this basis.

2. Confirming of Mechanism Type and Engraving Machine's Size

2.1 Selection of Mechanism Type and Coordinate System

The selection of mechanism type is the first step for designing novel engraving machine, the following reasons make us select the 6-PUS parallel mechanism for designing our engraving machine. Comparing with traditional mechanism, 6-PUS parallel mechanism uses base platform, three uprights layout and high rigidity framework structure and has the merits such as high modularization, high accuracy and low cost. Its model is shown in Fig.1.

As shown in Fig.1, 6-PUS parallel mechanism consists of base platform, dynamic platform and 6 branch chains with same structure, every branch joins with base platform through prismatic pairs (P), slider of prismatic pairs joins with up end of the fixed length link through universal joint (U) down end of the fixed length link joins with dynamic platform

through sphere hinge (S), so it is called 6-PUS parallel mechanism.
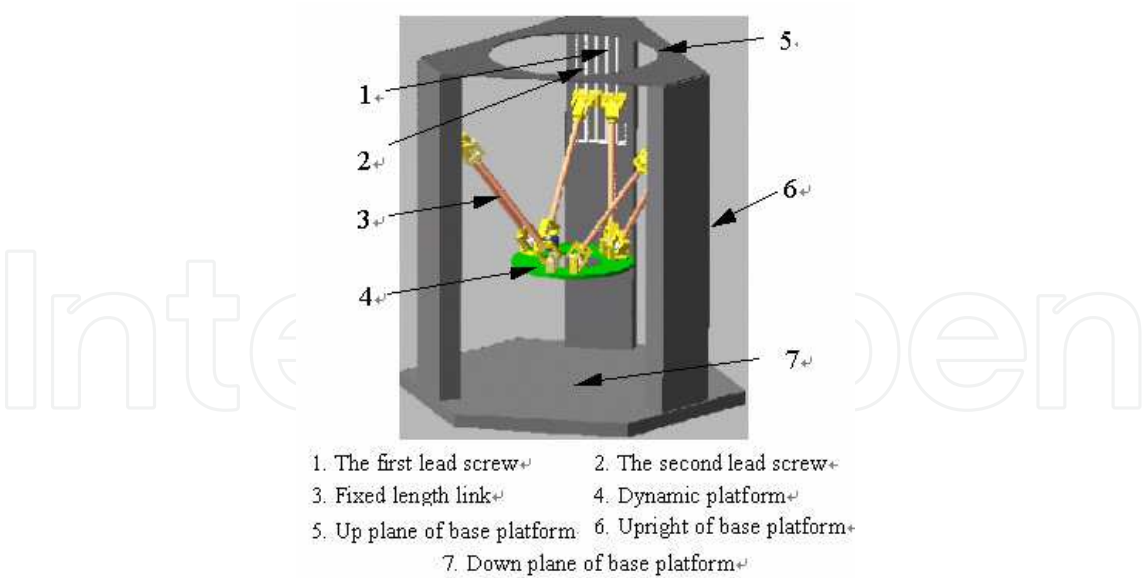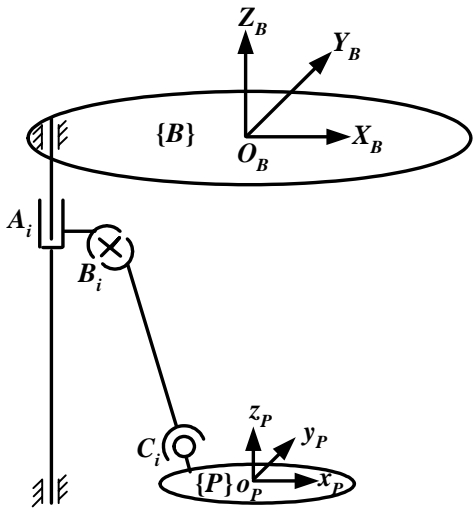

Figure 1. The model of 6-PUS parallel mechanism

Figure 2. Coordinate system of 6-PUS parallel engraving mechanism

The coordinate system of 6-PUS parallel engraving mechanism is shown in Fig. 2.
In Fig.2, the geometry centers of base platform and dynamic platform plane are supposed as O_B and o_p respectively. In every branch, the centers of prismatic pairs, universal joint and sphere hinge are marked with Ai, Bi, and Ci (i=1,2,…,6) respectively. Coordinate system O_B-$X_BY_BZ_B$ is fixed on base platform, taking {B} as briefly. The origin of {B} lies on geometry center of base platform's up plane, axis Z_B is vertical with base platform and directs to up, axis Y_B directs to angle bisector of the first and second branch lead screw center line, and axis X_B can be determined with right-hand rule. Supposing the coordinate system set on dynamic platform is $o_p - x_p y_p z_p$, taking {P} as briefly, its origin lies on geometry center of dynamic platform, the initial state of dynamic platform system is consistent with that of base platform system completely. Supposing the coordinate of o_p is (00Z) in {B}, this configuration without relative rotation to every axis is the initial configuration of this mechanism, and Z changing with mechanism's size. On the basis of

coordinate system mentioned, we use influence coefficient theory and the actual parameters of this mechanism to calculate the first and the second order influence coefficient matrix of every branch under different configuration. Then, we can get the first and the second order integrated influence coefficient matrix $\left[G_q^H\right]_{6x6}$ and $\left[H_q^H\right]_{6x6x6}$ of the whole mechanism. The significance and detailed solution process for influence coefficient matrix is omitted here, for more information please refer (Huang et al., 1997).

2.2 Mechanism Performance Analysis Based on Influence Coefficient Matrix

The performance of engraving machine will change with its size. To find out the better size for all the performance indices of both kinematics and dynamics, we obtain a group of mechanisms by changing its parameters. These mechanisms' length of fixed length links (L) range between 45cm and 55cm (step is 1cm), radius of dynamic platform (R) range between 10cm and 20cm (step is 1cm). Other parameters of the mechanism are unchanging, so we get 121 mechanisms totally.

Taking these mechanisms as research object, we confirm the sample point for every mechanism in its workspace with algorithm PerformanceAnalysis, then calculate the first and the second order influence coefficient matrix in every point. Furthermore, calculate all the performance indices in every sample point and draw all the global performance atlas of 121 mechanisms ultimately. To describe conveniently, we abbreviate the first and the second order integrated influence coefficient matrix $\left[G_q^H\right]_{6x6}$ and $\left[H_q^H\right]_{6x6x6}$ to G and H, and use Gω , Hω and Gυ, Hυ as the angular velocity submatrix and linear velocity submatrix of the first and the second order integrated influence coefficient matrix respectively, namely, $G = \left(\dfrac{G_\omega}{G_v}\right)$ and $H = \left(\dfrac{H_\omega}{H_v}\right)$.

Description for algorithm PerformanceAnalysis:

PerformanceAnalysis
 Begin
  For *L*=45 To 55   //scope of fixed length link
   For *R*=10 To 20   //scope of radius of dynamic platform
    SamplePointNumber=0 // initialization sample point number is zero for every mechanism
    For *x*= -Maximum To +Maximum moving along Axis *X*   Step 4cm
     For *y*=-Maximum To +Maximum moving along Axis *Y*   Step 4cm
      For *z*= -Maximum To +Maximum moving along Axis *Z*   Step 4cm
       For *α*= -Maximum To +Maximum rotating around Axis *X*   Step 12°
        For *β*=-Maximum To +Maximum rotating around Axis *Y*   Step 12°
         For *γ*=-Maximum To +Maximum rotating around Axis *Z*   Step 12°
          If sample point(*x, y, z, α, β, γ*)reachable point of mechanism's workspace
           Calculating the first order influence coefficient matrix and
           its Frobenius norm at current point ;
          If   The first order influence coefficient matrix is not singular
           SamplePointNumber= SamplePointNumber+1;
           Calculating the second order influence coefficient matrix
           and its Frobenius norm
           calculating condition number at this point with formula
           and accumulating sum of performance indices;
           //detailed formula is given in the following of this section
          Endif
         Endif
        Endfor
       Endfor
      Endfor
     Endfor

```
                    Endfor
              Endfor
              Calculating all the performance indices of the mechanism at current size and append the results
              to corresponding data files for different performance index;
              //performance index of the mechanism =
              (accumulating sum of performance indices at all sample points)/ SamplePointNumber
              //There are six data files for performance indices totally: angular velocity, linear velocity,
                angular acceleration, linear acceleration, force and moment, inertia force
        Endfor
     Endfor
     Drawing all the global performance atlas of 6-PUS mechanism by all the index data files
     (Every data file includes the information of 121 mechanisms);
     //There are six performances atlas totally: angular velocity, linear velocity, angular acceleration, linear acceleration,
     force and moment, inertia force

  End
```

We can change mechanism's parameters and adjust variable's step in the algorithm PerformanceAnalysis to meet actual analysis.

The algorithm is programmed with MATLAB and the global performance atlases of 6-PUS mechanism are drawn (see Fig. 3 to Fig. 8), then the mechanism's performance is analyzed using the atlas.

Table 1 shows the results of sample point number (abbr. to SPN) for 121 mechanisms respectively, the fixed link length of mechanism with sequence number (abbr. to SN) 1 is 45cm, its radius of dynamic platform is 10cm, the fixed link length of mechanism with SN 121 is 55cm, its radium of dynamic platform is 20cm, the rest may be deduced by analogy.

SN	SPN	SN	SPN	SN	SPN	SN	SPN	SN	SPN
1	30962	15	26874	29	20492	43	13852	57	52794
2	28074	16	23906	30	17530	44	11516	58	47350
3	25848	17	21026	31	14848	45	52222	59	42390
4	23252	18	18252	32	12466	46	47554	60	37410
5	20816	19	15784	33	10422	47	43064	61	32446
6	18368	20	13376	34	46608	48	38090	62	27818
7	16168	21	11304	35	42654	49	33780	63	23586
8	13824	22	9464	36	38406	50	29516	64	19902
9	11936	23	41324	37	34386	51	25254	65	16442
10	10106	24	37446	38	30214	52	21500	66	13696
11	8490	25	34194	39	26674	53	18098	67	63950
12	35554	26	30464	40	22830	54	15154	68	58034
13	32872	27	27038	41	19510	55	12570	69	52506
14	29628	28	23648	42	16410	56	58068	70	46696

SN	SPN	SN	SPN	SN	SPN	SN	SPN
71	41040	85	27942	99	17136	113	72098
72	35562	86	23204	100	81766	114	63828
73	30592	87	19196	101	74616	115	56058
74	25994	88	15858	102	66882	116	48546
75	21628	89	75848	103	59488	117	41388
76	17898	90	68936	104	52150	118	34892
77	14718	91	62052	105	45198	119	28942
78	69740	92	55164	106	38610	120	23998
79	63616	93	48462	107	32468	121	19828
80	57254	94	41880	108	27122		
81	50898	95	35792	109	22328		
82	44428	96	30158	110	18462		
83	38696	97	25188	111	88256		
84	33070	98	20736	112	79990		

Table 1. The SPN of 121 mechanisms in experiment

In addition, table 2 gives the performance indices of some mechanism only, where the mean of SN is same as in table 1.

SN	SPN	six performance indices					
		angular velocity	linear velocity	angular acceleration	linear acceleration	Force and moment	inertia force
1	30962	0.17276	0.17442	0.06236	0.11315	0.01521	0.37454
2	28074	0.18248	0.18171	0.08075	0.13276	0.01456	0.40421
3	25848	0.19128	0.18836	0.09932	0.15184	0.01396	0.43136
4	23252	0.20087	0.19545	0.11897	0.17225	0.01348	0.46030
…	…	…	…	…	…	…	…
59	42390	0.21105	0.18995	0.10050	0.15604	0.01304	0.40233
60	37410	0.21915	0.19537	0.11308	0.17355	0.01257	0.42606
61	32446	0.22717	0.20041	0.12312	0.19230	0.01216	0.44929
…	…	…	…	…	…	…	…
119	28942	0.25779	0.20680	0.12265	0.22596	0.01064	0.47030
120	23998	0.26786	0.21185	0.12116	0.24139	0.01041	0.49500
121	19828	0.27714	0.21610	0.11399	0.25527	0.01017	0.51745

Table 2. Six performance indices of some mechanism

2.2.1 Analysis of Kinematics Performance Indices

2.2.1.1 Global Performance Indices of Angular Velocity and Linear Velocity

As the influence coefficient G of engraving mechanism is not a constant matrix it makes the measuring index for parallel mechanism based on G not to be a constant matrix also, so we can't utilize one value to measure the good or bad of the dexterity, isotropy and controlling accuracy(Guo,2002). Here, we define parallel mechanism global performance indices of angular velocity and linear velocity as following respectively

$$\eta_{G_\omega} = \frac{\int_W \frac{1}{K_{G_\omega}} dW}{\int_W dW} \quad \text{and} \quad \eta_{G_v} = \frac{\int_W \frac{1}{K_{G_v}} dW}{\int_W dW} \tag{1}$$

Where W is the reachable workspace of mechanism, $K_{G_\omega} = \|G_\omega\| \|G_\omega^+\|$ and $K_{G_v} = \|G_v\| \|G_v^+\|$ denote the condition numbers for angular velocity and linear velocity respectively (Where $\|\cdot\|$ denotes Frobenius norm of matrix, superscript '+' denotes generalized inverse matrix, the same mean as following).We can get the performance indices' value of the angular velocity and linear velocity according to the condition numbers of every mechanism's sample points. Replacing the underlined part in algorithm PerformanceAnalysis with two formulas in (1) respectively, we can draw the performance atlas for angular velocity and linear velocity as shown in Fig.3 and fig.4 based on 121 mechanisms' indices values of angular velocity and linear velocity. According to the rule that the bigger $\eta_J (J \in \{G_\omega, G_v\})$,the higher dexterity and controlling accuracy of the mechanism, from Fig.3 we can see that the mechanism performance index of angular velocity is not changing with the link length when the changing range of R is not big, but it has the trend that the bigger R, the better performance index of angular velocity, furthermore, the index of mechanism angular velocity is better when L=46.5cm~49.5cm

633

and R=19.5cm, namely, the output error of angular velocity is smaller. Similarly, from Fig.4 we know that the mechanism index of linear velocity is better when L=45cm~48cm and R=19cm, that is to say, the output error of linear velocity is smaller.
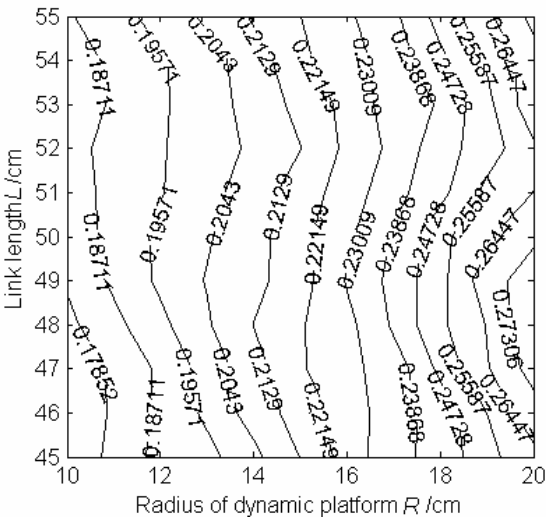

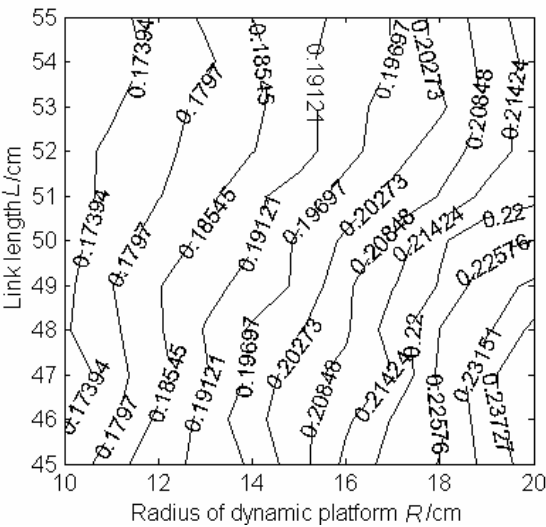Figure 3. Atlas of angular velocity global performance

Figure 4. Atlas of linear velocity global performance

2.2.1.2 Global Performance Indices of Angular Acceleration and Linear Acceleration

Considering the influences on acceleration of both the first and the second order influence coefficient matrix, the condition numbers of angular acceleration and linear acceleration for 6-DOF parallel mechanism are(Guo,2002; Guo & Huang,2002)

$$K_{G_\omega + H_\omega} = b\|G_\omega\|\|G_\omega^+\| + (a^2 + 2a)\|H_\omega\|\|H_\omega^+\| \tag{2}$$

$$K_{G_\upsilon + H_\upsilon} = b\|G_\upsilon\|\|G_\upsilon^+\| + (a^2 + 2a)\|H_\upsilon\|\|H_\upsilon^+\| \tag{3}$$

Where, a and b is error coefficient.

So the global performance indices of angular acceleration and linear acceleration for parallel engraving mechanism can be defined as

$$\eta_J = \frac{\int_W \frac{1}{K_J} dW}{\int_W dW} \tag{4}$$

Where $J \in \{G_\omega + H_\omega \pounds G_\upsilon + H_\upsilon\}$.

634

Supposed the mechanism error is smaller than 2%(that is, a=b=0.02), replacing the underlined part in algorithm PerformanceAnalysis with formula (4), we can draw the performance atlas for angular acceleration and linear acceleration as shown in Fig.5 and Fig.6. As same as the evaluating method for velocity performance index, from Fig. 5 we can see that the angle acceleration performance of mechanism is better when nearly L=45cm~47cm and R=16cm~20cm, output error is smaller accordingly. Among the 121 mechanism we studied, its maximum is 0.16399. By observing Fig.6 carefully, we know that performance of linear acceleration is better when nearly L=45cm~48cm and R=19.5cm, accordingly, output error should be smaller.
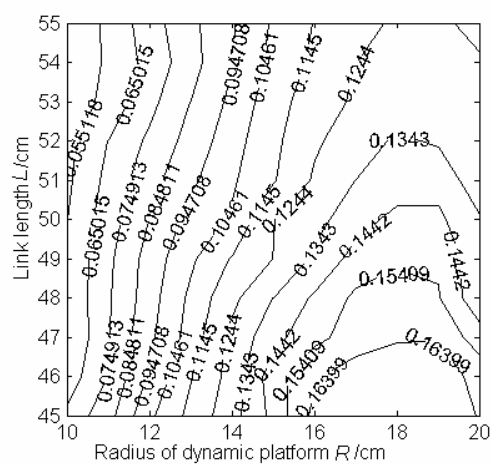

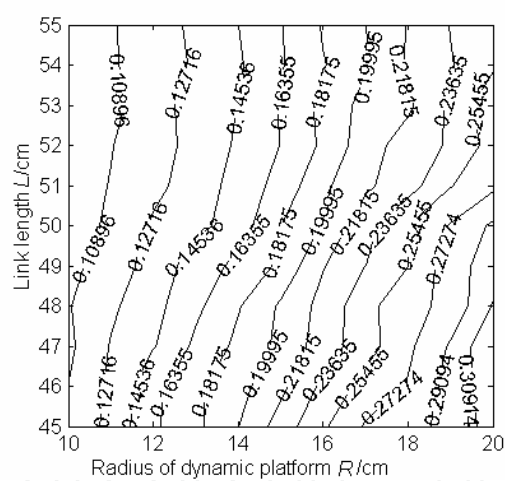Figure 5. Atlas of angular acceleration global performance

Figure 6. Atlas of linear acceleration global performance

From above analysis, we know that mechanism size with good indices for linear velocity and linear acceleration is coincidence in some degree among the 121 mechanisms we studied, but performance index of angular velocity and angular acceleration may not the best in the same size, so it can't get coincidence. Thus, our analysis will be helpful for designing and choosing mechanism by actual needs. Similarly, analyzing method of kinematics performance indices is the same when other parameters of the mechanism are changed.

2.2.2 Analysis of Dynamics Performance Indices

2.2.2.1 Analysis of Power and Moment Performance Index

The condition number of power and moment performance index based on the first order influence coefficient matrix of power G^F for 6-DOF parallel mechanism can be defined as

(Guo,2002)

$$K_{G^F} = \left\| G^F \right\| \left\| G^{-F} \right\|$$ (5)

Similarly, we define global performance index of power and moment for 6-DOF parallel mechanism as

$$\eta_{G^F} = \frac{\int_F \frac{1}{K_{G^F}} dW}{\int_F dW}$$ (6)

We suppose that power and moment of parallel mechanism is isotropy when $\eta_J=1$. With formula (5) as condition number, replacing the underlined part in algorithm PerformanceAnalysis with formula (6), we can draw the performance atlas for power and moment as shown in Fig.7. From Fig. 7 we can see in the size range of our experiment the performance index for power and moment would have little change with the link length when the radius of dynamic platform is less then 14cm. The performance index for mechanism's power and moment will be bigger when L=45cm~46cm and radius of dynamic platform R=10cm,here, performance of power and moment will be better.
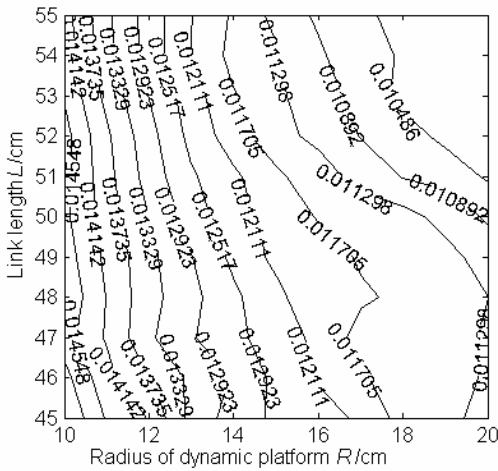

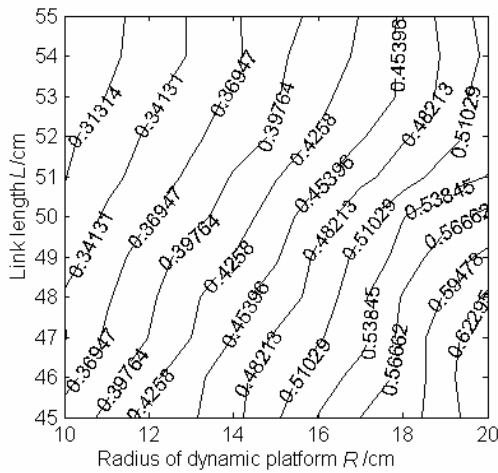Figure 7. Atlas of global performance of force and moment

Figure 8. Atlas of global performance of inertia force

2.2.2.2 Analysis of Inertia Force Performance Index

Considering both the first and the second order influence coefficient matrix, the condition number of inertia force for 6-DOF parallel mechanism is defined as(Guo,2002)

$$K_{G+H} = \sqrt{6}((\|G\| + \|H\| + (\|[G_\omega]_1\| + \|[G_\omega]_2\| + \|[G_\omega]_3\|)\|G_\omega\|))$$ (7)

Where $[G_\omega]_i$ is the ith column of matrix G_ω, i=1,2,3.

Then global performance index of engraving mechanism's inertia force can be defined as

$$\eta_{G+H} = \frac{\int\limits_W \frac{1}{K_{G+H}} dW}{\int\limits_W dW} \tag{8}$$

Obviously, the bigger value of η_{G+H}, the smaller inertia force of mechanism and the higher controlling accuracy. Replacing the underlined part in algorithm PerformanceAnalysis with formula(8), we can draw the performance atlas for inertia force as shown in Fig.8. According to the rule that the bigger value of η_{G+H}, the smaller inertia force of mechanism and the higher controlling accuracy, by observing Fig. 8 carefully, we can see that the inertia force performance index of mechanism is getting better when the link length is getting longer and radius of dynamic platform is getting bigger. Furthermore, the inertia force performance index of mechanism will be the best when nearly L=45cm~48cm and R=19.5cm, that is to say, the inertia force performance of mechanism is the best, inertia force is the smallest, sensitivity is the best and dexterity is the highest.

According to discusses above, we draw a conclusion that mechanism size with good performance index for power and moment and inertia force is coincidence not in all the time. This result indicates that the traditional designing and choosing mechanism method based on only the first order influence coefficient exists some restriction, we have to choose mechanism size on the basis of our analysis and actual demands.

2.3 The Results of Size Design and Summary

Summarizing previous analysis, we know that 6-PUS robot mechanism's all performance indices are better except force and moment when L=45cm~47cm and R=19cm, the actual size of mechanism with this type owned by laboratory is at the above-mentioned scope. We also find that its performances are same with the results of theory analysis by running the mechanism in deed, so prove the correctness of our theory. To validate our theory analysis further, we also do lots of simulations for this mechanism with other sizes. The results are same with those of theory analysis, so we can draw the conclusion that, in a generally way, there is not a mechanism whose all indices are better at the same time for both the kinematics and dynamics. In fact, we can only select the mechanism with relative better performance for all the indices to meet our need. On the basis for considering all the performance indices, the final sizes of novel parallel engraving machine that we designed are following:

The length of fixed link L is 46cm, the radius of dynamic platform R is 19cm, the radius of base platform is 38cm, $\{\varphi_{P1},\varphi_{P2},\varphi_{P3},\varphi_{P4},\varphi_{P5},\varphi_{P6}\}=\{45°,135°,165°,255°,285°,15°\}$, $\{\phi_{B1},\phi_{B2},\phi_{B3},\phi_{B4},\phi_{B5},\phi_{B6}\}=\{82°,97°,202°,217°,322°,337°\}$, $\varphi_C=30°,\phi_A=15°$. Where φ_{Pi} (i=1,2,…6)is the angle between tieline from dynamic platform's center o_p to C_i and the axis x_p's positive direction of dynamic platform's coordinate system, ϕ_{Bi} (i=1,2,…6)is the angle between tieline from base platform's center O_B to A_i and the axis X_B's positive direction of base platform's coordinate system. φ_C and ϕ_A is the smaller central angle of hexagon made by C_i and A_i (i=1,2,…6) respectively.

3. Research on Path Planning of Engraving

A series of engraving paths can be obtained after the image of workpiece to be engraved is

dealt with image processing technology and tool path generating algorithm(Lo,1998), these paths consist of a series of straight line segments(exclusive for direction-parallel machining). When engraving on plane, the control of engraving path has the linear mapping relation to the cutting tool path that has been planned. But when engraving on spacial curved surface, the engraving path on plane should be mapped into the path on curved surface, this mapping is more complex than the former. In this section, we will pay attention to cutting tool path's mapping method from plane to spacial curved surface and the planning algorithm of cutting tool's posture.

3.1 Mapping Method of Cutting Tool Path

To describe conveniently, supposing the curved surface S to be engraved is

$$S = S(u,v) = \{x(u,v), y(u,v), z(u,v)\} \quad (u,v) \in D \tag{9}$$

Where D is one region on the uv plane.
Curve C on curved surface S can be expressed as

$$C = C(t) = S(u(t), v(t)) = \{x(t), y(t), z(t)\} \quad t \in [t_0, t_n] \tag{10}$$

Then arbitrary point Ci on curve C is

$$C_i = C(t_i) = \{x(t_i), y(t_i), z(t_i)\} = \{x_i, y_i, z_i\} \ (i = 0,1,\cdots,n) \tag{11}$$

In addition, supposing the image plane of workpiece to be engraved is superposition with coordinate system xOy that describes the curved surface S, then the plane equation describing workpiece image is

$$z = 0 \tag{12}$$

For one cutting tool path on plane with length of d, start and end point is $Ps(x_1,y_1,0)$ and $Pe(x_2,y_2,0)$ respectively, which should be mapped into a curve segment when engraving on spacial curved surface. Furthermore, the vertical projection's length of chord length corresponding to curved segment should equal with the straight line segment's length d. The line equation of plane cutting tool path's straight line segment can be expressed as

$$\begin{cases} x = x_1 + (x_2 - x_1)t \\ y = y_1 + (y_2 - y_1)t(-\infty < t < \infty) \\ z = 0 \end{cases} \tag{13}$$

The equation of plane P that passes plane cutting tool path's straight line segment and is vertical with image plane is

$$(y_2 - y_1)x - (x_2 - x_1)y - x_1 y_2 + x_2 y_1 = 0 \tag{14}$$

Then the intersecting line of plane P and curved surface S to be engraved is the curve C, on which is cutting tool path on curved surface crresponding to that on plane. By this, the start and end point's coordinates of cutting tool path on curved surface, which corresponding to that on plane, are Ps' (x_1,y_1,z_1) and Pe' (x_2,y_2,z_2) respectively, as x_1,y_1,x_2,y_2 are known, z_1 and z_2 can be deduced with equation (10). It is easy to validate that the cutting tool path's mapping method metioned above can suit for arbitrary quadrant of the coordinate system and engraving path in arbitrary direction.

3.2 Interpolation Computing of Spacial Curve

Real-time interpolation computing is necessary to engrave spacial curve segment, whose coordinates of start and end point are Ps' (x_1,y_1,z_1) and Pe' (x_2,y_2,z_2) respectively, with parallel engraving machine. Firstly, the interpolation number N should be calculated by interpolation precision, then the coordinates of ith interpolation point can be expressed as

(x_i, y_i, z_i), where $x_i = x_1 + \frac{x_2 - x_1}{N}i, y_i = y_1 + \frac{y_2 - y_1}{N}i.(i = 1,2,\cdots,N)$, z_i can be deduced with equation (10). When i=N, it shows the terminal Pe' of the curve segment. According to actual needs, many interpolation algorithms can be selected during engraving (Yang,2002).

3.3 Posture Planning of Cutting Tool

In view of the special structure of parallel mechanism and ensuring effect for engraving, the posture of cutting tool should be considered during engraving(Lee,1997), namely, the posture of cutting tool for every interpolation point should also be calculated besides its position during the control process. For parallel engraving machine with 6-DOF, the rotation around axis Z_B is not used in generally, the rotation angle α and β around axis X_B and Y_B will be solved in following.

Supposing the base coordinate system of parallel engraving mechanism in initial state is same with that of curved surface(curve), that is, the axial line of cutting tool of cutting tool is vertical with dynamic platform plane of engraving machine and fixed on it, then the rotation angles of dynamic platform plane around X_B and Y_B both are zero, namely, the angle between axial line of cutting tool and X_B and Y_B both are π/2, as shown in Fig.9(a).

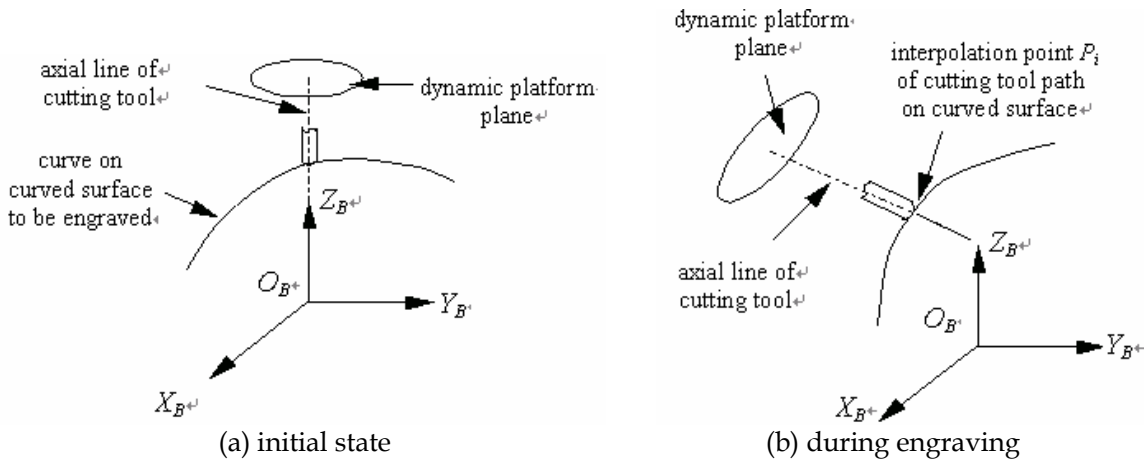(a) initial state   (b) during engraving
Figure 9. The sketch map of cutting tool's posture for initial state and during engraving

Without losing generality, now taking arbitrary interpolation point P_i (x_i, y_i, z_i) on curve as sample, as shown in Fig.9(b), then the tangent plane (parallel with the dynamic platform plane of engraving machine) equation of curved surface through point P_i can be expressed as

$$\begin{vmatrix} x - x_i & y - y_i & z - z_i \\ x_u^{'} & y_u^{'} & z_u^{'} \\ x_v^{'} & y_v^{'} & z_v^{'} \end{vmatrix} = 0 \tag{15}$$

Translating the general form as

$$Ax + By + Cz - (Ax_i + By_i + Cz_i) = 0 \tag{16}$$

Where

$A = y_u^{'}z_v^{'} - y_v^{'}z_u^{'}, B = z_u^{'}x_v^{'} - z_v^{'}x_u^{'}, C = x_u^{'}y_v^{'} - x_v^{'}y_u^{'}$

In addition, the line equation of axis X_B and Y is as following respectively

$$y=z=0 \text{ and } z=x=0 \tag{17}$$

According to the relation between spacial plane and line, the angle θ_x and θ_y, representing the angle between dyanmic platform plane of engraving machine and axis X_B and Y_B respectively, satisfy

639

$$\sin\theta_x = \frac{|Al_1 + Bm_1 + Cn_1|}{\sqrt{A^2 + B^2 + C^2} \cdot \sqrt{l_1^2 + m_1^2 + n_1^2}} = \frac{|A|}{\sqrt{A^2 + B^2 + C^2}} \quad (18)$$

$$\sin\theta_y = \frac{|Al_2 + Bm_2 + Cn_2|}{\sqrt{A^2 + B^2 + C^2} \cdot \sqrt{l_2^2 + m_2^2 + n_2^2}} = \frac{|B|}{\sqrt{A^2 + B^2 + C^2}} \quad (19)$$

In formula (18) and (19), l1;m1;n1 and l2;m2;n2 represent the parameters of symmetrical line eqution of axis X_B and Y_B respectively. Then we can get

$$\theta_x = \arcsin\frac{|A|}{\sqrt{A^2 + B^2 + C^2}}; \text{when A≥0 is } \theta_x; \text{otherwise } -\theta_x.$$

$$\theta_y = \arcsin\frac{|B|}{\sqrt{A^2 + B^2 + C^2}}; \text{when B≥0 is } \theta_y; \text{otherwise } -\theta_y.$$

Here, θ_x and θ_y represent the angle β and α, β and α is the rotation angle of dynamic platform plane rotating around axis Y_B and X_B respectively. Positive value denotes counterclockwise rotation, negative value denotes clockwise rotation. Thus, the posture parameter (α,β,0) of arbitrary interpolation point can be obtained, coupled with position parameter above, the position and posture of arbitray interpolation point on curve can be expressed as $P_i(x_i,y_i,z_i,\alpha,\beta,0)$. So it can be ensured that the axial line of cutting tool at arbitrary interpolation point will be vertical with the tangent plane of engraving point all the time.

3.4 Summary of Tool Path Planning

On the basis of preceeding work, table 3 gives the corresponding relationship between interpolation points of straight line cutting tool path on plane and that of curved surface in space.

		start point	interpolation point i	end point
cutting tool path on plane		$(x_1,y_1,0,0,0,0)$	$(x_i,y_i,0,0,0,0)$	$(x_2,y_2,0,0,0,0)$
cutting tool path on curved surface	tangent plane	$A(x-x_1)+B(y-y_1)+C(z-z_1)=0$	$A(x-x_i)+B(y-y_i)+C(z-z_i)=0$	$A(x-x_2)+B(y-y_2)+C(z-z_2)=0$
	position and posture	$(x_1,y_1,z_1,\alpha_1,\beta_1,0)$	$(x_i,y_i,z_i,\alpha_i,\beta_i,0)$	$(x_2,y_2,z_2,\alpha_2,\beta_2,0)$

Table 3. The corresponding relationship between cutting tool path on plane and curved surface

Based on the theory mentioned above, we simulate the cutting tool path on plane and spacial curved surface when engraving Chinese characters "mu", as shown in Fig.10

(a)tool path on plane   (b)tool path on parabolic cylinder   (c)tool path on sphere
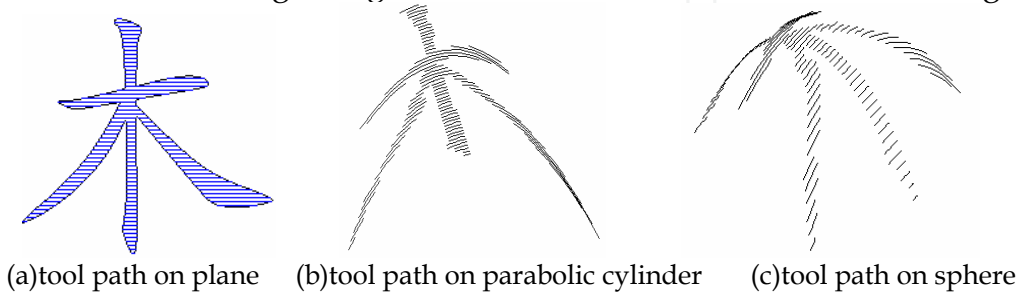
Figure 10. The sketch map of cutting tool path

This section mainly resolves some questions about parallel engraving machine engraves on arbitrary spacial curved surface which is expressed with parameter equation, then

realizes the mapping of cutting tool path from plane to spacial curve surface in the workspace of engraving machine. In addition, questions about interference and error analysis are not discussed in this section, the reason is that these questions will be involved only considering the radius of cutting tool, these works will be done in the future.

4. Research on Force Control Technology of Engraving Machine

Control technology for engraving machine can be classified two types: free motion control and constrained motion control. The control when the cutting tool of engraving machine does not contact with the workpiece is called free motion control. It is called constrained motion control when there is interaction between the cutting tool and the workpiece. Position control can meet demands when cutting tool of engraving machine moves in free space. Not only position but also contact force between cutting tool and environment should be controlled during engraving job. The aim of force control is to realize precise operation, but the first location in large scope is achieved by position control. As position control is relative simple and mature, this section will pay attention to the research on the technology of force control. At present, force control technology often used can be classified two types of basic and advanced. Basic force control technology also has two schemes: impedance control(Hogan,1985) and hybrid force/position control (Raibert & Craig,1981). Where, impedance is one force control technology developed in early stage, which does not control the force between machine and environment directly but control the dynamic relationship between force and position (or velocity) to implement force control. It is called impedance control because this dynamic relationship is similar to the concept of impedance in circuit. Hybrid force/position control is a scheme that implements force control and position control in "force subspace" and "position subspace" respectively, although its theory is definite, it is difficult to be realized. Basic control method of engraving force is simple and feasible, it also can achive better control effect when the enviroment parameters are invariable. The precision of basic force control technology depends on the mathematical model of the engrving machine totally as this method's patameters are invariable. We have deduced the accurate dynamics model of engraving machinism in (Kong et al., 2004) as follow

$$SF=K \tag{20}$$

Where

$$S = \begin{bmatrix} {}^P s^1 & {}^P s^2 & {}^P s^3 & {}^P s^4 & {}^P s^5 & {}^P s^6 \\ {}^P r^1 \times {}^P s^1 & {}^P r^2 \times {}^P s^2 & {}^P r^3 \times {}^P s^3 & {}^P r^4 \times {}^P s^4 & {}^P r^5 \times {}^P s^5 & {}^P r^6 \times {}^P s^6 \end{bmatrix}$$

$$F = \left(\left\| \frac{{}^P F_{d1}^1}{\left({}^P s^1\right)^T {}^P b^1} \right\| \quad \left\| \frac{{}^P F_{d1}^2}{\left({}^P s^2\right)^T {}^P b^2} \right\| \quad \left\| \frac{{}^P F_{d1}^3}{\left({}^P s^3\right)^T {}^P b^3} \right\| \quad \left\| \frac{{}^P F_{d1}^4}{\left({}^P s^4\right)^T {}^P b^4} \right\| \quad \left\| \frac{{}^P F_{d1}^5}{\left({}^P s^5\right)^T {}^P b^5} \right\| \quad \left\| \frac{{}^P F_{d1}^6}{\left({}^P s^6\right)^T {}^P b^6} \right\| \right)^T$$

$$K = \begin{pmatrix} m\,{}^P\dot{v} + m\,{}^P g - {}^P F_E + 6\sum_{n=1}^{3} m_n\,{}^P g + \sum_{i=1}^{6}\sum_{n=1}^{3} m_n\,{}^P\dot{v}_{cn}^i \\ {}^P I_P\,{}^P\dot{\omega}_P + {}^P\omega_P \times {}^P I_P\,{}^P\omega_P + \sum_{i=1}^{6}\left[{}^P r^i \times \sum_{n=1}^{3} m_n\left({}^P\dot{v}_{cn}^i + {}^P g\right) \right] - {}^P r_E \times {}^P F_E - {}^P M_E \end{pmatrix}$$

Please refer (Kong et al., 2004) for the meanings of all variables in formula (20). According to formula (20), the driving forces for appointed task can be solved when the kinematics parameters and engraving force and moment are known. But as the uncertainty of environment during actual engraving process, conventional method can't be adjusted

641

effectively when parameters are changed, so good control effect can't be obtained, then it is not suitable for the control of engraving machine. Along with the development of control technology, many researchers introduce advanced control technology to robot force control methods, which causes the appearance of advanced force control technology such as adaptive fuzzy control and neural network(NN) control etc. Fuzzy logic is similar to the thinking approach of human and more suitable for dealing with the uncertain and non-linear issues. Neural network is suitable for parallel computing and has the function of adaptive learning etc. Combining the merits of fuzzy control and neural network technology, fuzzy neural network(FNN) control makes the fuzzy control parameters and rules to be adjusted, modified and perfected automatically during control process, then the control performances of system can be improved constantly and the best control effect can be achieved finally. The control method of engraving force based on FNN technology proposed by us will be discussed in the following.

4. 1 The Structure and Learning Algorithm of FNN

We adopt five-layer NN to implement the fuzzy reasoning rules. The five layers are input layer, fuzzified layer, fuzzy association layer, fuzzy postassociation layer and output layer. In the five layers, the nodes of input layer is connected directly to the components of input vector and transports the input values to the next layer. Fuzzified layer completes the calculation of membership function and realizes the fuzzification of input variables, so every node of this layer corresponds to one linguistic variable. Every node of fuzzy association layer represents one fuzzy rule, which is used to match the antecedent of fuzzy rule and calculate the applicable degree of every rule. To given input, the value of linguistic variable only near the input point has bigger membership degree. Fuzzy postassociation layer completes normalized calculation, which prepares for the reasoning process of next layer. Output layer accomplishes defuzzification and outputs concrete value of the FNN. Generally speaking, NN should to be trained before practical application. For engraving machine, its engraving environment is not fixed commonly, the learning result of network for a certain environment is not suitable for other environment usually, so it needs retraining to adapt the new system. Therefore, online learning and adaptive ability is very important to the control of engraving force. Only the output layer has weight in our FNN, and only the local connect weights, which are connected with the activated neurons, are adjusted. The supervised Hebb learning rule(it is a learning algorithm without tutor) is adopted in this paper, which uses the deviation between desired force and actual force as supervised signal, and adjust the position by self-organizing and self-learning to environment information through associated searching, then realizes the tracking of desired engraving force finally.

4.2 The Design of Force Controller

Control framework of engraving force for parallel engraving machine based on FNN is shown in Fig.11, where the concrete structure of FNN is 2-14-49-49-1.
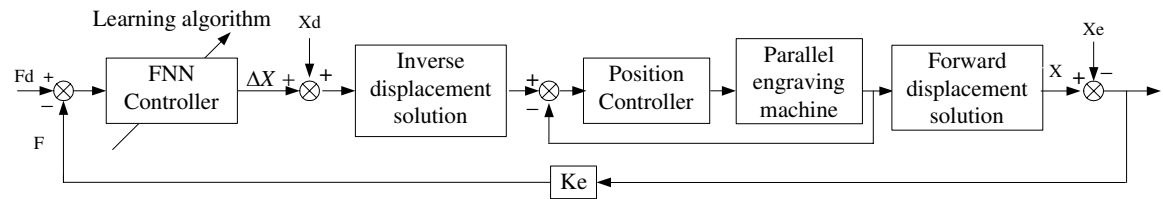

Figure 11. Control framework of engraving force for parallel engraving machine based on FNN

642

In Fig.11, FNN controller uses force error F_e and error changing rate $\dot{F}_e$ as input value, position adjustment ΔX as output value where $F_e \in [-1000\text{N},1000\text{N}], \dot{F}_e \in [-10000\text{N}/s,10000\text{N}/s], \Delta X \in [-0.01\text{m},0.01\text{m}]$. F_d is desired force trajectory, F is the actual engraving force. K_e is stiffness matrix of engraving enviroment, which is commonly a positive diagonal matrix, that is to say, the eviroment is decoupled in all directions. X_d is desired position trajectory. X is the actual position of engraving machine's cutting tool. X_e is the position when the engraving enviroment is not deformed. Fuzzy subsets about input and output linguistic variable of fuzzy controller both are negtive large(NL), negtive middle(NM), negtive small(NS), zero(ZE), positive small(PS), positive middle(PM) and postive large(PL), the following bell function is used as membership function

$$\mu_{ij} = \exp\left\{-\frac{(x_i - \sigma_{ij})^2}{\delta_{ij}^2}\right\}, \quad (i = 1,2 \quad j = 1,2,\cdots,7) \tag{21}$$

Where σ_{ij} and δ_{ij} is the center and width of membership function respectively. Fuzzy control rule is shown in Table 4.

$\dfrac{F_e}{\dot{F}_e}$	NL	NM	NS	ZE	PS	PM	PL
NL	NL	NL	NM	NL	NS	ZE	PS
NM	NL	NL	NM	NL	NS	PS	PM
NS	NL	NL	NM	NL	PS	PM	PL
ZE	NL	NL	NS	ZE	PM	PL	PL
PS	NL	NM	NS	PL	PL	PL	PL
PM	NM	NS	ZE	PL	PM	PL	PL
PL	NS	NS	PS	PL	PL	PL	PL

Table 4. Fuzzy control rule

Fig.12 to Fig.19 are the simulation results in one direction of degree-of-freedom (which can represent arbitrary direction) based on the control method mentioned above. Where dashed line shows desired engraving force, solid line shows actual engraving force.
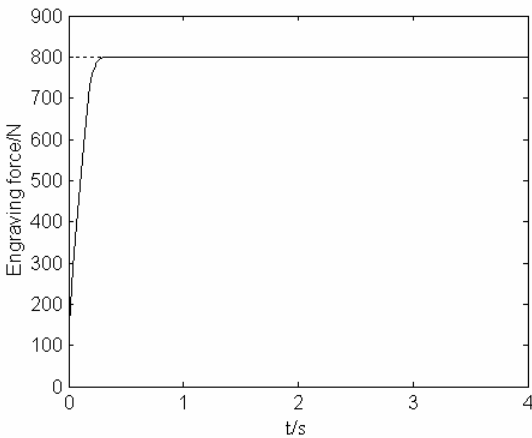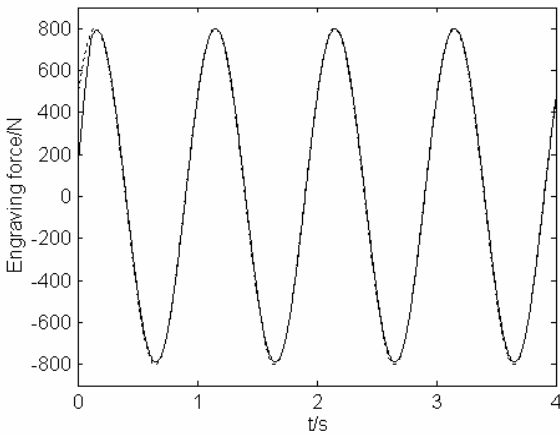

Figure 12. Response of step force with 800N

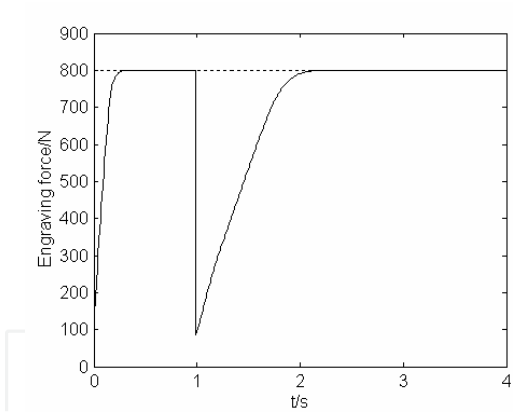Figure 13. Response of time-changing force with 800sin(2пt+п/5)

Figure 14. Response of step force under environmental stiffness changing (when *t*=1, *Ke* changing from 10000N/m to 1000N/m)
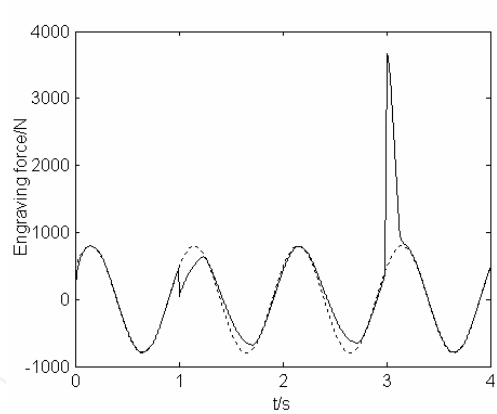

Figure 15. Response of sine force under environmental stiffness changing (when *t*=1, *Ke* changing from 10000N/m to 1000N/m, and *t*=3, *Ke* changing from 1000N/m to 10000N/m)
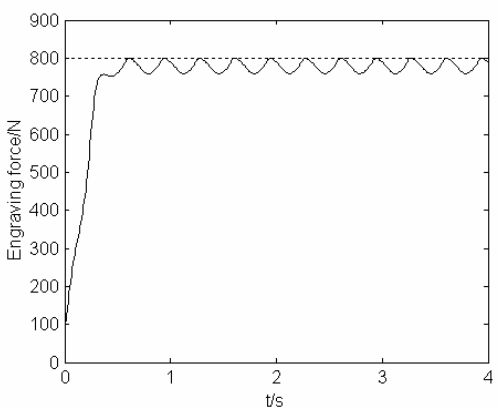

Figure 16. Response of step force under environmental position changing ($Xe = 0.005 \left| \sin(3\pi t + \frac{\pi}{4}) \right|$)
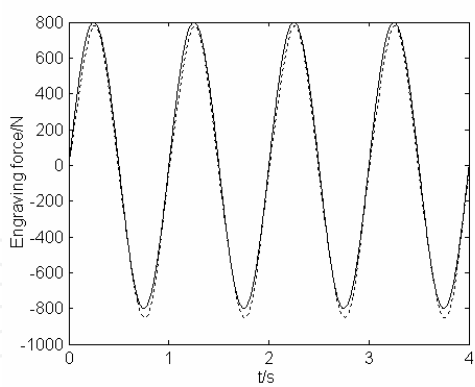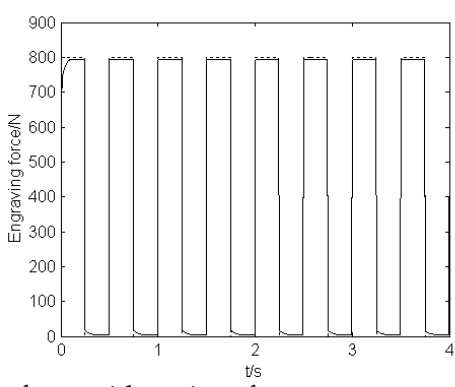

Figure 17. Response of sine force under environmental position changing $Xe = 0.005 \left| \sin(3\pi t + \frac{\pi}{4}) \right|$)

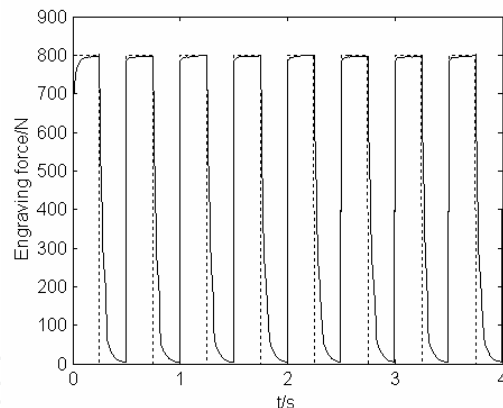Figure 18. Response of squarewave force without interference

644

Figure 19. Response of squarewave force with noise(0,10)

From above results, we draw the conclusion that the control technology of engraving force based on FNN can make adjustment rapidly according to the changing of environment parameters, the whole system has merits such as rapid response to new environment, small influence by changing parameters, strong adaptability and robustness.

5. Research on Teleoperation Technology for Parallel Engraving Machine Based on B/S Mode

5.1 Implementation of Teleoperation System

The structure of teleoperation system for parallel engraving machine is shown in Fig.20, which adapts supervised control model(Huang & Mak,2001). This kind of control model makes operator out of the closed loop for control structure, so the influence on the whole system by transmission delay is decreased. Three parts functions, i.e. motion control, engraving control and video feedback, are provided to the use by web server. Motion control mainly implements the motion of engraving machine such as straight line, circular arc, ellipse and pentagon etc. Engraving control implements related task about actual engraving, including input of information to be engraved, contour extraction, tool path generation, machining simulation and actual engraving, which is the control core of parallel engraving machine and decides the engraving effect. The running state can be monitored real-time by starting the function of video feedback during process of both motion control and engraving control. All functions mentioned above can be shared by multiuser except controlling the engraving machine.
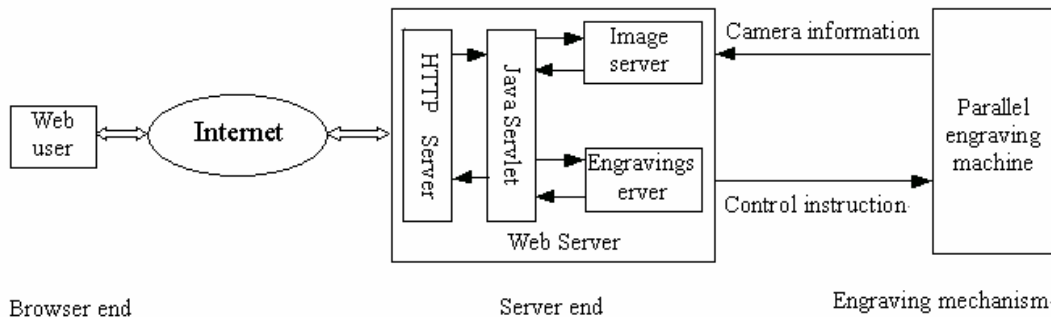

Figure 20. The structure of teleoperation system

The mutual exclusion principle between progress is adopted in our system to avoid sharing engraving machine by multiuser at the same time. The detailed method can be described as follow. A common variable is used as semaphore, every web user will test the

state of this variable before actual engraving. "0" represents that the engraving machine can be controlled, "1" represents does not and now the related prompting message such as "system is busy" will be send to user immediately. Once the engraving machine is controlled by one user, the common variable will be assigned to "1" and other users will not use the machine, so the reliability of system can be guaranteed. Engraving task may be canceled by the user for all kinds of reasons during engraving process, which asks the control algorithm for engraving machine have the ability to respond new instruction during control. This question can be resolved by setting a common variable like above, what the control program should do is to test the value of this variable every time before sending control instruction to engraving machine. In addition, to ensure that only the user who submits the job has qualification to terminate engraving task, the system will return a unique ID to the browser end after engraving task is submitted successfully. The system will ask the user to submit a ID when user want to terminate engraving task and will compare the ID provided by user with the ID of task being executed. The engraving job will be terminated if the two IDs are coincident, otherwise the system will warn that the user has not the privilege to terminate the task. The Java Media Framework(JMF) is adopted for real-time transmission of video information. JMF is the application program interface for streaming media developed by SUN, through which the multimedia function is introduced to Java. As Remote Transport Protocol(RTP) has been implemented in JMF, the real-time acquisition and transmission of video information can be realized with JMF easily.

5.2 Experiments for Teleoperation

To verify the feasibility of our system, the engraving of straight line, circle, ellipse and pentagon is implemented successfully firstly, on this basis, the engraving of Chinese characters also successes by visiting the engraving server through local area network. In addition, remote engraving and real-time transmission for video information is obtained success further by visiting server through Internet. Fig.21 shows the system interface for engraving Chinese characters "zi". Fig.22 shows the parameters to be submitted for straight line motion of engraving machine, here the "engraving control" part on the right side of Fig.21 will change into the content of Fig.22, similar as "circular arc motion" and other functions.

Figure 21. The interface of teleoperation system for engraving

Figure 22. The submitted parameters for straight line motion

6. Conclusions

A novel parallel engraving machine is proposed and its some key technologies are studied in this paper. Based on the confirming of mechanism type, a group of mechanisms are obtained by changing the sizes of engraving machine. Performance indices are analyzed by considering both the first and the second order influence coefficient matrix of different sample point in every mechanism's workspace, then mechanism's sizes better for both kinematics and dynamics are achieved, so the theory basis for designing the size of novel engraving machine is established. In addition, method for tool path planning and control technology for engraving force is also studied in the paper. The proposed algorithm for tool path planning on curved surface solves path's mapping method from plane to spacial curved surface, which can be applied to arbitrary curved surface in theory. Control technology for engraving force based on FNN also has strong adaptability to the unknown environment. The implementation of teleoperation for parallel engraving machine based on B/S mode can meet the demands of distance engraving for ordinary web user, which also can be expanded to other machining domain besides engraving, so long distance and network machining can be realized. Simulation experiments are done based on the proposed model of engraving machine and related methods, simulation results show the feasibility and validity of the proposed methods. Beneficial exploration has been done for further design and development of future novel engraving machine in the paper.

7. References

Guo,X.J.(2002). Research on Dynamical Basal Theory of Parallel Robotic Mechanism. Dissertation for the Doctoral Degree in Engineering of Yanshan University,China

Guo, X.J. & Huang,Z.(2002). Analysis for Acceleration Performance Indices of Parallel Robots. China Mechanical Engineering,13(24): 2087-2091,ISSN 1004-132X

Huang,G.Q.&Mak, K.L.(2001).Web-integrated Manufacturing: Recent Developments and Emerging Issues. International Journal of Computer Integrated

Manufacturing,14(1):3-13,ISSN 0951-192X

Huang,Z.; Kong,L.F. & Fang, Y. F.(1997). Mechanics Theory and Control of Parallel Robot. Publishing House of Machinery Industry, ISBN 7-111-05812-7, Beijing, China

Hogan ,N.(1985). Impedance Control: An Approach to Manipulation: Part I-theory. Part II-Implementation. Part III-Applications. ASME Journal of Dynamic Systems, Measurement, and Control, 107:1-24, ISSN 0022-0434

Kong, L.F.; Zhang,S.H.; Xiao,W.H..; Li, C.Y.& Huang, Z.(2004). Rigid Body Dynamics Model of the 6-PUS Parallel Mechanism Based on Newton-Euler Method. Robot, 2004,26(5):395-399,ISSN 1002-0446

Lee, Y.S.(1997). Admissible Tool Orientation Control of Gouging Avoidance for 5-Axis Complex Surface Machining. Computer-Aided Design, 29(7): 507-521,ISSN 0010-4485

Lo,C.C.(1998)A New Approach to CNC Tool Path Generation. Computer-Aided Design, 30(8): 649-655,ISSN 0010-4485

Raibert, M.H. & Craig, J.J. (1981). Hybrid Position/Force Control of Manipulators. ASME Journal of Dynamic Systems, Measurement, and Control,102: 126-133, ISSN 0022-0434

Taylor,K.& Dalton,B.(2000). Internet Robots: a New Robotics Niche. IEEE Robotics & Automation Magazine,7(1):27-34, ISSN 1070-9932

Yang, X.N.(2002). Efficient Circular Arc Interpolation Based on Active Tolerance Control. Computer-Aided Design, 34(13): 1037-1046, ISSN 0010-4485

Yao, Y.X. & Lu Y.(1999). Research on Remote Working Condition Information Integration Based on Computer Network. Aeronautical Manufacturing Technology,42(1):13-17,ISSN 1000-8756

Cutting Edge Robotics

Edited by Vedran Kordic, Aleksandar Lazinica and Munir Merdan

ISBN 3-86611-038-3

Hard cover, 784 pages

Publisher Pro Literatur Verlag, Germany

Published online 01, July, 2005

Published in print edition July, 2005

This book is the result of inspirations and contributions from many researchers worldwide. It presents a collection of wide range research results of robotics scientific community. Various aspects of current research in robotics area are explored and discussed. The book begins with researches in robot modelling & design, in which different approaches in kinematical, dynamical and other design issues of mobile robots are discussed. Second chapter deals with various sensor systems, but the major part of the chapter is devoted to robotic vision systems. Chapter III is devoted to robot navigation and presents different navigation architectures. The chapter IV is devoted to research on adaptive and learning systems in mobile robots area. The chapter V speaks about different application areas of multi-robot systems. Other emerging field is discussed in chapter VI - the human- robot interaction. Chapter VII gives a great tutorial on legged robot systems and one research overview on design of a humanoid robot.The different examples of service robots are showed in chapter VIII. Chapter IX is oriented to industrial robots, i.e. robot manipulators. Different mechatronic systems oriented on robotics are explored in the last chapter of the book.

How to reference

In order to correctly reference this scholarly work, feel free to copy and paste the following:

INTECH
open science | open minds